

A Study of the Cycle-to-Cycle Variation of In-Cylinder Flow on a Motored Engine

L.Zhang, T.Ueda, T.Takatsuki and K.Yokota

*Isuzu Advanced Engineering Center Ltd.
8 Tsuchidana Fujisawa Kanagawa 252
Japan*

ABSTRACT

An experimental study investigating the cyclic variation of the internal air motion has been made in a motored engine having a cup-in-piston combustion chamber. The engine used for this study has a transparent quartz liner and a transparent plastic (acrylic resin) piston. The light source used to produce sheet was a 4 watt argon ion laser with continuous wave beam. The brightness irregularity patterns of particle groups were recorded photographically by a NAC E-10 high speed camera and the bulk flow fields inside of the combustion chamber have been measured at both planes parallel and vertical to the piston crown by means of image processing technique.

This paper for the first time reveals the continuous cycle-resolved two-dimensional bulk flow fields inside of the combustion chamber around the compression TDC. Also, comparison between cycle-resolved and ensemble-averaged flow patterns has shown that ensemble-averaged flow pattern may become a artificial one if there exists the large effect of the cyclic variation. Moreover, by examining into the rms of the variation component and the ratios of the rms to ensemble-averaged velocity under with/without swirl conditions, it is found that the ratios of the rms to ensemble-averaged velocity can be used for evaluating the effect of the cyclic variation on the flow fields.

INTRODUCTION

Since the in-cylinder flow has strong influence on both spark ignition and compression ignition engines[1], much insight into these flow fields has been gained by flow visualization and by using LDV measurements(e.g.[2-5]). These results of previous works have shown the flow field inside of the combustion chamber are unsteady with a wide range of spatial and temporal fluctuations. However, the LDV measurements are limited to single point or along a line, the entire cycle-resolved structure of the flow field and how these flow fields would be affected by the cyclic variation remain unclear.

Recently, multi-point velocity measurements of the flow field have become available in engines by using particle tracking velocimetry, PTV[6] and particle image velocimetry,PIV,[7][8]. Some of the

results have shown there may have strong cyclic variation effects on the flow field[9][10]. However, these works only obtained isolated flow fields at one time(crank angle) in many individual cycles, the lack of continuous results of the flow fields in time series make it confusion whether these phenomena were caused by high or low frequency fluctuations, namely the variations or turbulence.

On the other hand, the numerical simulations that can deal with cyclic variation have shown some significant cycle-to-cycle changes among the flow fields[11][12]. These results of numerical simulations also need verification.

Therefore, in order to make clear the phenomena of the cyclic variation and its effect on the flow fields, more experimental research is highly desirable.

EXPERIMENTAL

ENGINE-A DI Diesel engine was remodeled into a research engine fitted with transparent extended piston and cylinder liner, available for optical access to both planes of parallel and vertical to the piston crown inside of the combustion chamber as shown in Figure 1. Table 1 gives the major specifications of this engine. The combustion chamber geometry was a centered, cylindrical cup-in-piston configuration, 15mm in height and 40mm in diameter(Figure 2).

For this study, the engine was motored at constant speed of 500 rpm. Two heads with the port swirl ratios (namely the value of the swirl tester) of 0 (without swirl) and 2.4 (with swirl) were used. The visualized plane parallel to the piston crown was fixed 10mm below the cylinder head and the plane vertical to the piston crown was formed by a laser sheet from the exhaust valve to the intake valve through the cylinder axis. The flow was seeded with the particles (Expancel 091DE, 70 μ mean diameter and 0.025 mean density) which are estimated to follow fluctuations of below 100Hz[13].The particles were introduced into the flow by a seeder, attached to the intake port.

VISUALIZATION SYSTEM-A 4 watt, continuous wave argon ion laser was used to produce the sheets

* Numbers in brackets designate references at end of this paper

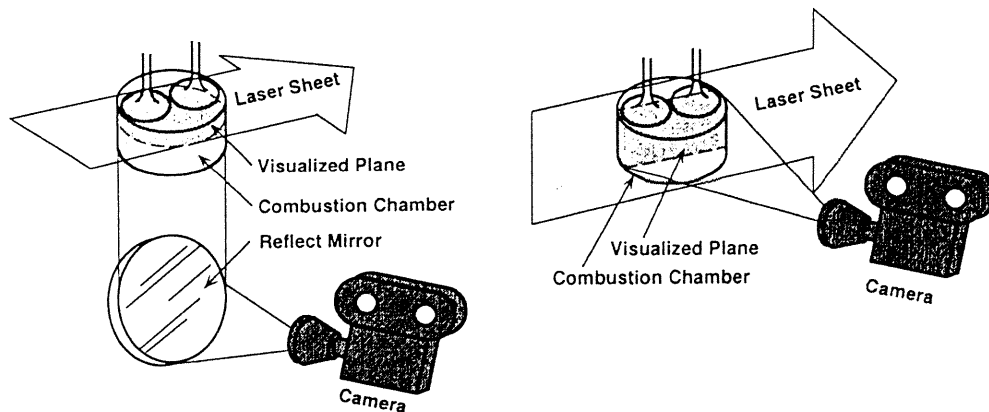


Figure 1: Schematic of the visualization planes parallel to the piston crown (left) and vertical to the piston crown (right) inside of the combustion chamber

Table 1: Major Engine Specifications

Type of Engine	Single Cylinder 4-Stroke
Valve	One Inlet /One Exhaust
Bore×Stroke	$\phi 82 \times 78 \text{ mm}$
Displacement	411 cm^3
Comp. Ratio	13.5
Top Clearance	1.0 mm
Port Swirl Ratio	0/2.4

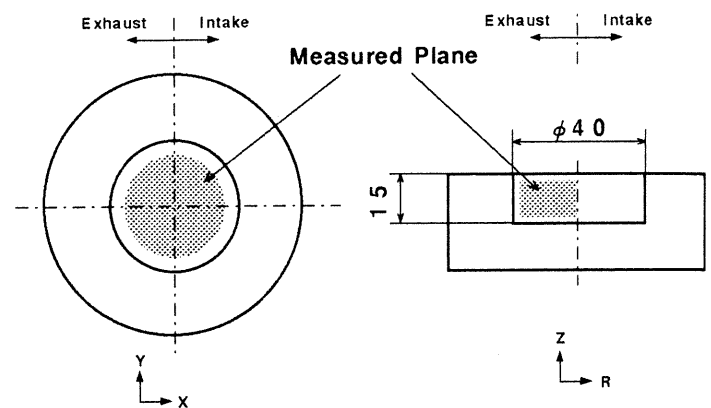


Figure 2: Chamber geometry and processing area at both planes. The x and y directions of the parallel plane, the r and z directions of the vertical plane are indicated.

necessary for the experiment. The laser beam was focused into sheets aligned parallel or vertical to the piston crown by two cylindrical lenses. The laser sheet thickness was measured to be 8mm. A NAC E-10 high speed camera was used to sequentially record the brightness irregularity patterns of the particle groups on Kodak 7222 film. A Nikon f1.4 50mm lens was used for the vertical plane case and another Nikon f1.8 105mm lens was used for the parallel plane. The magnification factor of the images recorded in this experiments was 0.15 for the vertical plane and 0.11 for the parallel plane.

The procedure for recording the photographs was first to make the engine speed stable, than send a signal both to the seeder to seed the flow and to the camera to start recording. The recording speed was 2000fps for the condition of without swirl and 3000fps for the swirl condition, respectively.

PROCESSING METHOD—Films which has photographed the brightness irregularity patterns of the particle groups were input into a computer by a NAC film motion analyzer and NAC ID8000 system(512 × 512 pixels, 8

bit). The separate images at time t and $t + \Delta t$ are then cross correlated with each other to produce an unambiguous displacement vector. The displacement vector divided by the time interval of Δt gives the velocity at one correlating area. A velocity resolution of this system is 0.26m/s per pixel for the vertical plane and 0.5m/s per pixel with swirl and 0.34m/s per pixel without swirl for the parallel plane.

Theoretically, if one correlation area has more than two patterns, the smaller the size of correlation area the better the spatial resolution can be expected. However, practically, the correlation area was decided by try and error method. In this study, by minimizing the size of the area on condition of controlling the illegal vectors below 10% on two typical images[14], the size of the correlation area was previously decided as 24×24 pixels matrix.

A vector was regarded as an illegal vector if it was not within tolerance of its four nearest neighbors average velocity[14-16]. When an illegal vector was found, the vector was replaced by re-

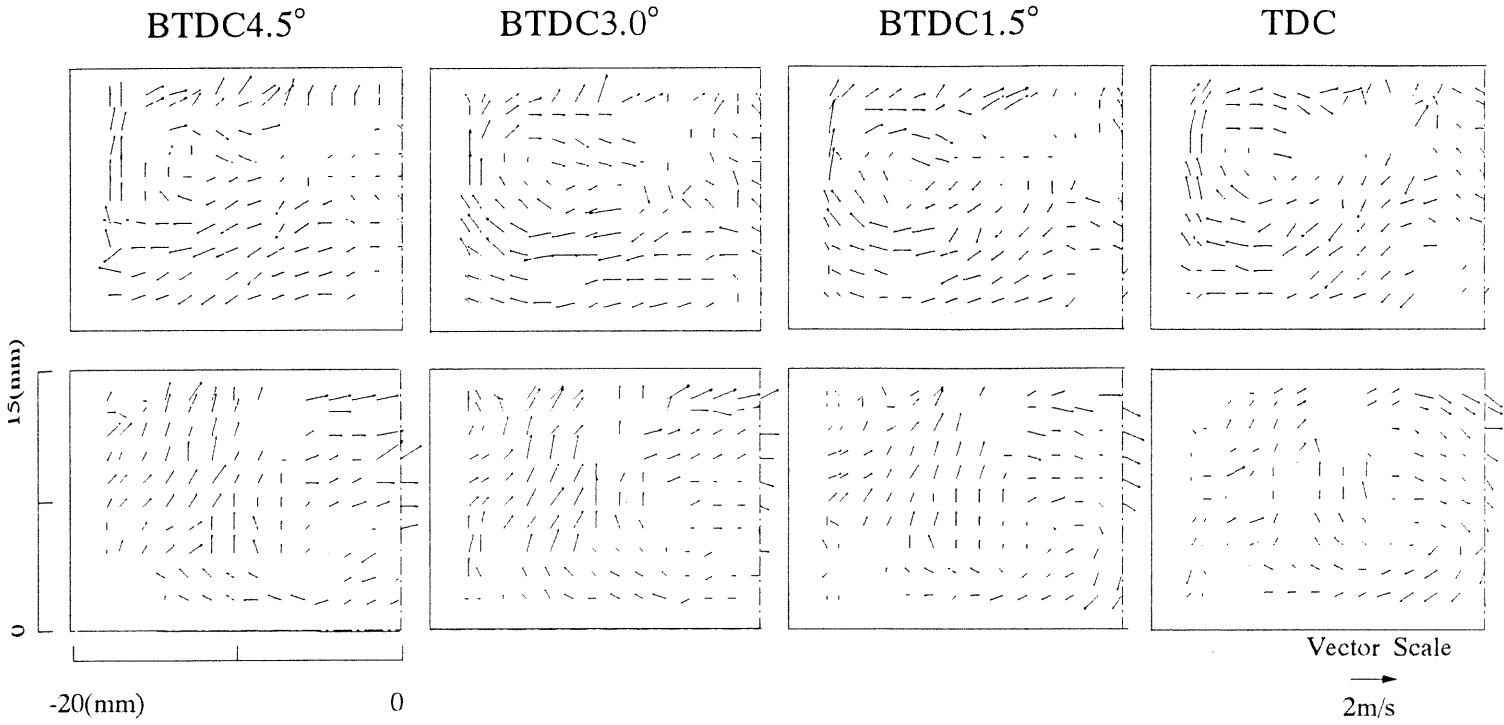


Figure 3: Sequence of any two cycle-resolved flow fields (top and bottom represent different cycles) at the vertical plane without swirl, from BTDC4.5° to TDC. The results showed the right hand half of the chamber (see fig.2, the dotted lines represent the center axis. The solid lines represent the chamber profile).

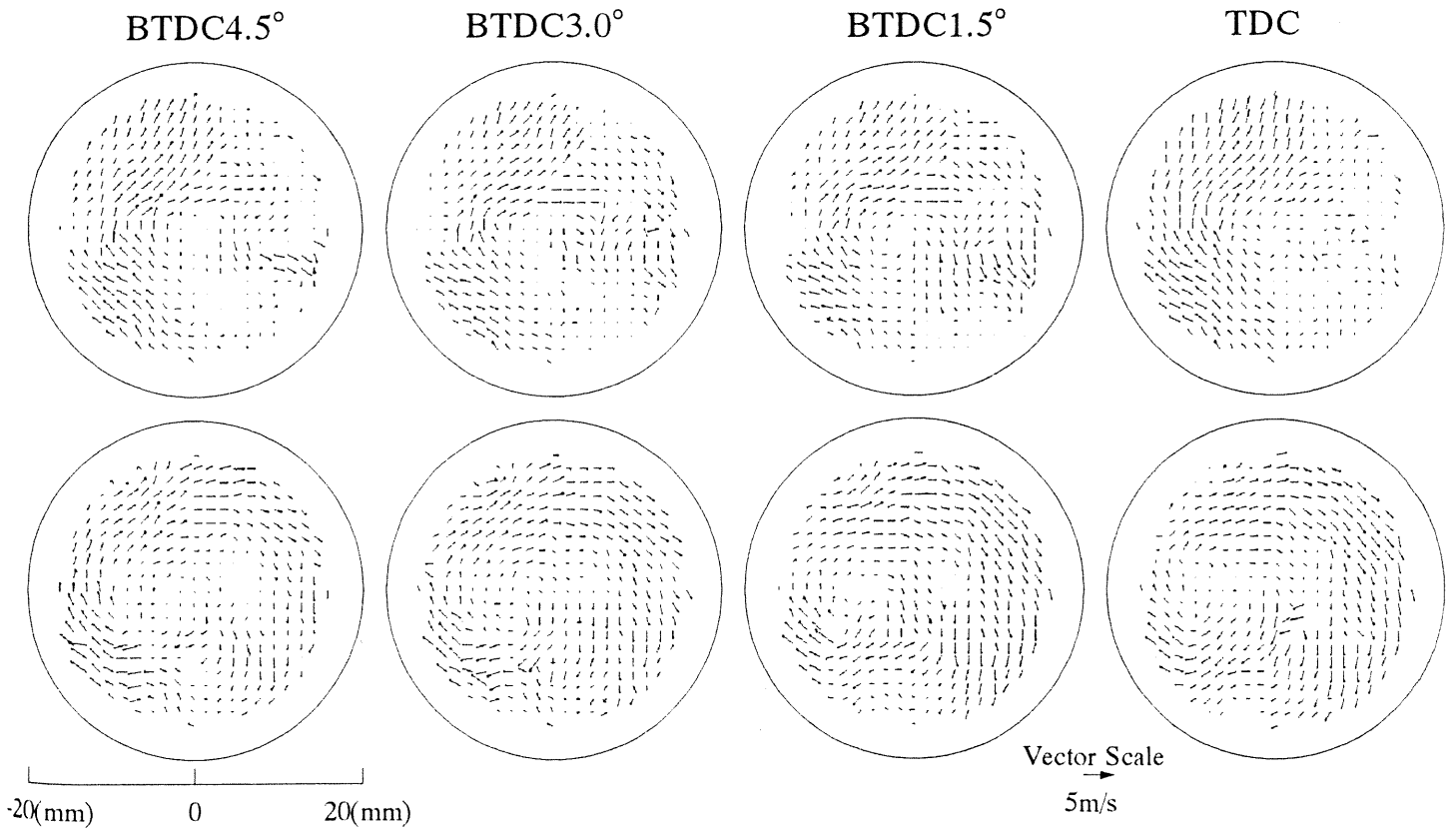


Figure 4: Sequence of any two cycle-resolved flow fields (top and bottom represent different cycles, the circular solid lines represent the chamber outline) at the parallel plane without swirl, from BTDC4.5° to TDC.

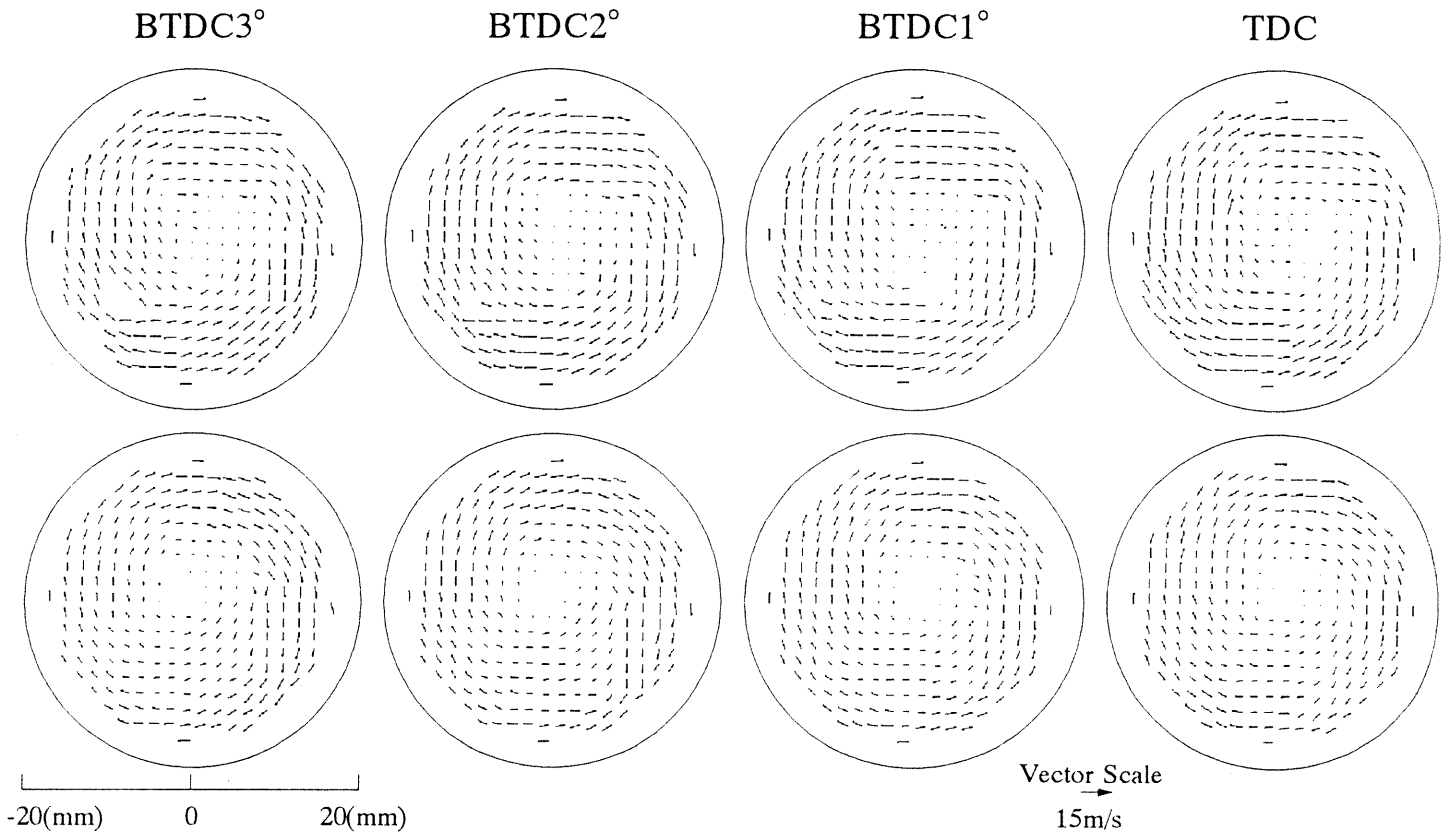


Figure 5: Sequence of any two cycle-resolved flow fields (top and bottom represent different cycles, the circular solid lines represent the chamber outline) at the parallel plane with swirl, from BTDC3° to TDC.

calculated vector based on the enlarged matrix with 36×36 pixels. Even after this process there remained very few bad vectors, these vectors were deleted manually. Therefore, there were still some areas where the vector was still blanked.

Although the image of the particles observed as a brightness irregularity pattern and the use of the high speed camera result in relatively low spatial and temporal resolution as compared with the PIV, the advantage of ease measurement procedure and of producing continuous flow fields make it suitable for the purpose of this study.

The processing areas at both planes are also shown in Figure 2.

RESULTS AND DISCUSSION

CYCLE-RESOLVED AND ENSEMBLE-AVERAGED FLOW PATTERN—Figure 3 and Figure 4, respectively, give any two continuous cycle-resolved two-dimensional flow fields without swirl from BTDC 4.5° to TDC at both planes. The velocity vectors represented by arrows, show the direction and magnitude of the velocity. Comparing each continuous cycle-resolved two-dimensional flow fields at both planes, pronounced differences among the structures of the flow fields caused by velocity fluctuations were observed. Meanwhile, since the measurement and particles used in

this study would not be expected to catch the high-frequency fluctuations and each cycle of the above figures showed a sequence of similar flow patterns without instantaneous changes, apparently the velocity fluctuations observed in these cases were primarily the low-frequency fluctuations of the cyclic

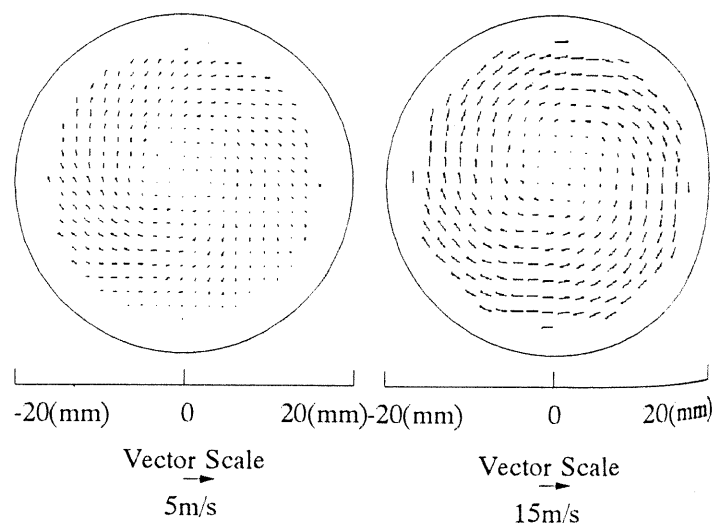


Figure 6: Ensemble-averaged (25 cycles) flow patterns of the TDC under with swirl (right) and without swirl (left) conditions.

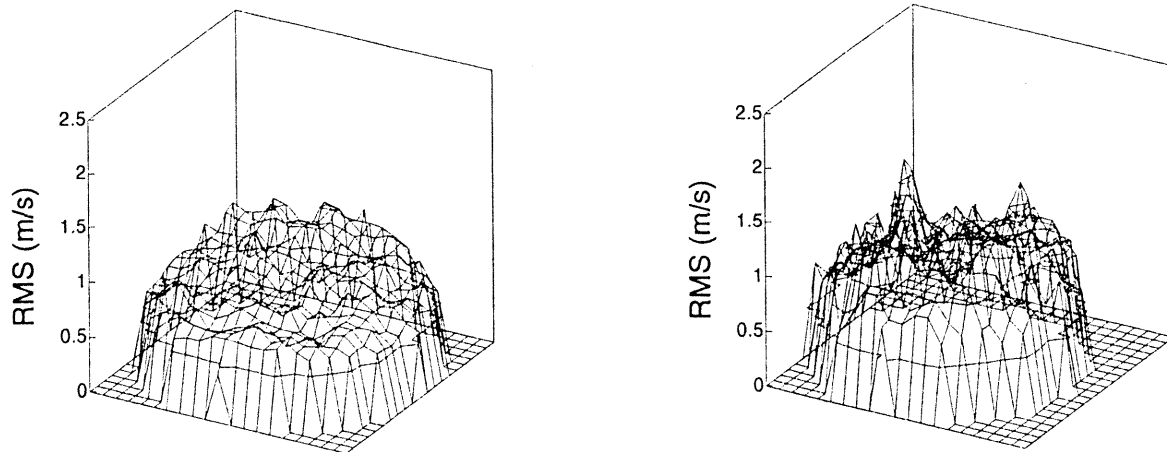


Figure 7: RMS distribution of the TDC at the parallel plane with(right)/without(left) swirl (25 cycles). RMS was defined as $(RMS_t^2 + RMS_r^2)^{0.5}$; RMS_t is the tangential component; RMS_r is the radial component.

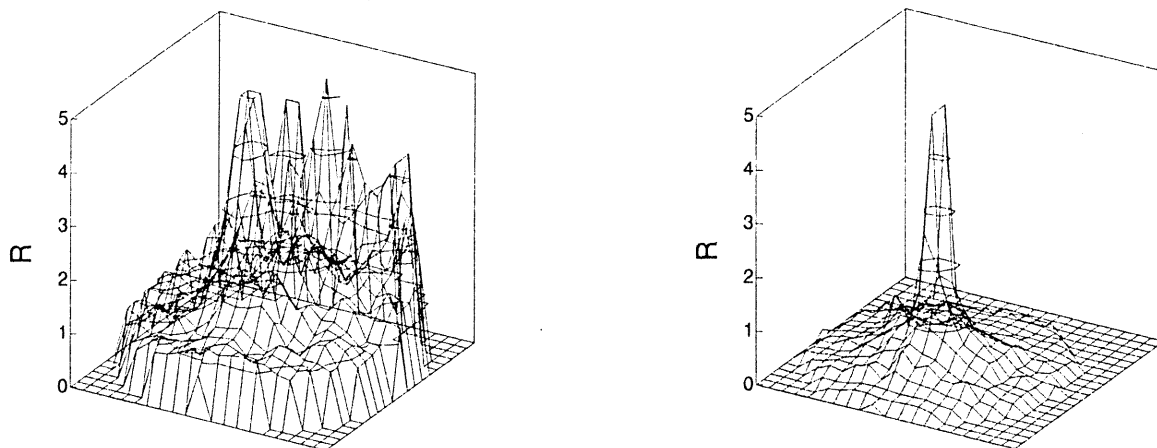


Figure 8: Ratios of the RMS to the ensemble-averaged velocity with(right)/without(left) swirl as represented by letter R, at the TDC. The ensemble-averaged velocity is defined as $(v_t^2 + v_r^2)^{0.5}$; v_t is the tangential component; v_r is the radial component.

variations. Therefore, the concern that these fluctuations may be caused by high-frequency fluctuations, that is the turbulence was excluded. As a result, it was concluded that the fluctuations of the flow fields were resulted from the cyclic variation.

Another comparison of the continuous cycle-resolved two-dimensional flow fields between any two cycles with swirl from BTDC 3° to TDC at the plane of parallel to the piston crown is shown in Figure 5. In this case, the flow fields were almost shown the similar pattern exception that the center of the swirl changed location from one cycle to the next.

The ensemble-averaged flow fields with/without swirl of the TDC at the parallel plane are shown in Figure 6. Comparing the cycle-resolved flow patterns of the TDC in Figure 4 and 5 with the ensemble-averaged flow patterns of the TDC in Figure 6, the difference is clear. If the cycle-resolved flow fields were almost similar as shown in Figure 5, the

ensemble-averaged flow field was also similar to the cycle-resolved flow field. However, if the cycle-resolved flow fields largely fluctuate between each other as in Figure 4, as expected, the ensemble-averaged flow field of Figure 6 became a artificial field, none of the real flow fields can be represented.

CHANGES IN RMS AND RATIOS OF RMS TO ENSEMBLE-AVERAGED VELOCITY—In order to evaluate the effect of the cyclic variation on the structure of the flow field, first of all, the rms of the variation component at the parallel plane with/without swirl were compared in Figure 7. Despite of the different behaviors of the flow patterns in each case, there has no evident difference between its rms, indicating the evaluation would be difficult if only rely on rms itself. Furthermore, since the magnitude of the ensemble-averaged velocity changes in a wide range as shown in Figure 6, even if there are the same rms,

the effects of the rms on the flow field may result in different ways. That is, the magnitude of ensemble-averaged velocity should be counted also to evaluate the effects of the cyclic variation, namely the rms. Therefore, the authors associate the rms with the ensemble-averaged velocity by using the ratios of the rms to the value of ensemble-averaged velocity to evaluate the effects of the rms. Figure 8 show the results at the same planes of Figure 7 as an example to see how the ratios are changed in different cases. Here, the ratios of the rms to the value of ensemble-averaged velocity are represented by letter R in the vertical axis of Figure 8. Comparing each other in Figure 8, the values of the R under the swirl condition were smaller than the values without swirl. Under the swirl condition, the values of the R were almost below 1 exception the center area, in where the possibility of appearing swirl center is high. However, in the case of without swirl, the values of the R larger than 1 were dominated in the plane. Where the values of the R are larger than 1 means the rms, that is the flow variations become the main component that dominate the flow field, resulted in a large fluctuation in the flow patterns. Therefore, the use of the values of the R, that is the ratios of the rms to the value of ensemble-averaged velocity can give an evaluation of the similarity between cycle-resolved and ensemble-averaged structures of the flow field and the effect of the cyclic variation on the flow fields under different conditions.

In addition, this study indicates there needs more caution to explain the results obtained by means of ensemble-averaged method in the case of existing flow variation.

CONCLUSIONS

The application of multi-measurement technique to a motored engine has revealed for the first time the continuous cycle-resolved two-dimensional bulk flow fields inside of a cup-in-piston combustion chamber around the compression TDC. The comparison between individual cycles shows that the flow cyclic variation has strong influence on the structures of the flow field. The conclusions of this study are as follows:

(1) The two-dimensional and time serial structures of the bulk flow fields inside of the combustion chamber around the compression TDC have been revealed.

(2) There has strong effect of the flow variation on cycle-resolved flow patterns, in some cases of this study, these patterns fluctuate significantly from cycle to cycle.

(3) When the flow fields fluctuate largely, the ensemble-averaged flow field can not represent the real structure of the flow field.

(4) Use of the ratios of the rms to the value of ensemble-averaged velocity, the similarity between

cycle-resolved and ensemble-averaged structures of the flow field and the effect of cyclic variation on the flow field can be evaluated.

REFERENCES

- [1] J.B.Heywood, "Internal Combustion Engine Fundamentals," McGraw-Hill Book Co., New York, 1988.
- [2] R.B.Rask, "Laser Doppler Anemometer Measurements of Mean Velocity and Turbulence in Internal Combustion Engines," In Intl.Conf.on Applics.of lasers and Electro-Optics, Boston, Nov.12-15,1984.
- [3] T.D.Fansler et al., "Cycle-resolved Laser-velocimetry Measurements in a Reentrant-bowl-in-piston Engine," SAE paper 880377,1988.
- [4] T.M.Liou et al., "LDV Measurements in Valved and Ported Engines," SAE paper 840375,1984.
- [5] A.R.Glover et al., "An Investigation into Engine Turbulence Using Scanning LDV," SAE Paper 880379,1988.
- [6] W.Hentschel et al., "Flow Visualization with Laser Light-Sheet Techniques in Automotive Research," In C.Veret, editor, Flow Visualization IV, Hemisphere Pub.Corp., Washington,1987.
- [7] D.L.Reuss et al., "Instantaneous Planar Measurements of Velocity and Large-Scale Vorticity and Strain Rate in an Engine Using Particle-Image Velocimetry," SAE Paper 890616,1989.
- [8] D.L.Reuss et al., "Velocity, Vorticity and Strain-Rate Ahead of a Flame Measured in an Engine Using Particle Image Velocimetry," SAE Paper 900053,1990.
- [9] E.Nino et al., "Two-Color Particle Image Velocimetry in an Engine with Combustion," SAE paper 930872,1993.
- [10] K.Kawahara et al., "Three-Dimensional In-Cylinder Flow Field Structure Measurement by Three-Color Laser Light sheet Method," In Proc.of the 11th Internal Combustion Engine symposium,Tokyo,Japan,1993.
- [11] K.Naitoh et al., "Large Eddy Simulation of Turbulence Premixed-Flame in Engine by using the Renormalization Group Theory and the Multi-Level Formulation," Trans.of JSME, 59-559,B(1993-3),953.
- [12] Y.Hamai et al., "A Two-Dimensional Computer Simulation of Cycle-to-Cycle Flow Variation Inside a Rotary Engine System," In Proc.of the 11th Internal Combustion Engine symposium,Tokyo,Japan,1993.
- [13] H.Kato et al., "3-D PTV measurement of an air turbulence flow," Journal of the Visualization Society of Japan, Vol.12, No.1, pp111,1992.
- [14] L.Zhang et al., "In-Cylinder Flow Measurement by Cross-Correlation Method," to be published on Trans. of JSAE.
- [15] M.Maeda, "Simultaneous and Time Series Measurements of Two-Dimensional Velocity and Temperature Fields Using an Image Processing Technique," Proc.14th IEA Task Leaders Meeting, pp259,1992.
- [16] D.C.Bjorkquist et al., "Particle Image Velocimetry," In ATLAS OF VISUALIZATION, Progress in Visualization Vol.1, 1992, pp313, PERGAMON PRESS,1993,TOKYO.